Sensors & Transducers, Vol. 255, Issue 1, January 2022, pp. 17-23

www.sensorsportal.com

Sensors & Transducers

Published by IFSA Publishing, S. L., 2022
http://www.sensorsportal.com

Laser Ranging and Nudging in Space Debris Traffic Management

[1, *] Claude Phipps and [2] Christophe Bonnal

[1] Photonic Associates, LLC, 200A Ojo de la Vaca Rd., Santa Fe NM 87501, USA
[2] CNES, 52 rue Jacques Hillairet 75612, Paris Cedex, France
[1] Tel.: +1-215-358-4360, fax: +1-505-466-3877
E-mail: crphipps@aol.com

Received: 13 December 2021 /Accepted: 17 January 2022 /Published: 31 January 2022

Abstract: The number of satellites in LEO is dramatically increasing, from single objects 60 years ago to a predicted 100,000 in 2030. U.S. companies have requested approval for 58,000 new satellites in the next decade, 42k from SpaceX alone. Each week, 3k LEO objects pass each other closer than 1km. In 2018, the European CAESAR conjunction assessment system handled 3M conjunction messages leading to only 17 effective maneuvers. The problem is the low precision with which we know the orbits of these objects. Improving that precision by a factor of 100 will reduce the annual number of false collision alarms to an acceptable level. Just-in-time Collision Avoidance (JCA) can prevent anticipated collisions, given improved ephemeris precision. In this paper we show how this can be done with a 100 ps laser ranging network and one or a few laser nudging stations in orbit. We will discuss the components of this system, as well as an eight-year plan for implementation.

Keywords: JCA, ps laser, Laser ranging, Laser nudging, Space debris traffic management.

1. Introduction

Fig. 1 shows the exponentially growing number of debris in low Earth orbit (LEO). Within the next decade an additional 60 k satellites are expected to be approved, most of which will belong to the SpaceX Starlink system [1] plus additional satellites from other similar planned systems. By 2050, 600 k objects larger than 1cm are predicted to populate LEO [2]. In 1978, Kessler [3] predicted that mutual debris collisions would soon become the largest source of new debris. This is now the case (Fig. 2), as a result of 35 years of bad space housekeeping, which has led to about 10,000 tons of LEO space debris. Space is a commons: trashing it is a disaster that can ultimately trap us on this planet.

In space, no fatalities have occurred yet, but there have been several incidents, including one in November, 2021, in which the International Space Station (ISS) astronauts were forced to abandon the Station and seek protection inside their attached re-entry vehicles. International cooperation is essential to solve the debris problem. In orbit, typical impact velocity is 12 km/s due to the variety of launch latitudes and inclinations. At this velocity, debris have several times the energy density of dynamite.

Despite the fact that SpaceX has designed its satellites to re-enter, the sheer number on orbit will surely lead to more collisions than we have seen in the past. Each week, 3k LEO objects pass each other closer than 1 km [4]. Just-in-time collision avoidance (JCA) [5] can prevent anticipated collisions, but anticipation depends on better orbit ephemeris precision. Laser ranging can improve the present precision by a factor of 100, which leads to a collision false alarm rate of about 100/year, to about 0.02/year [6].

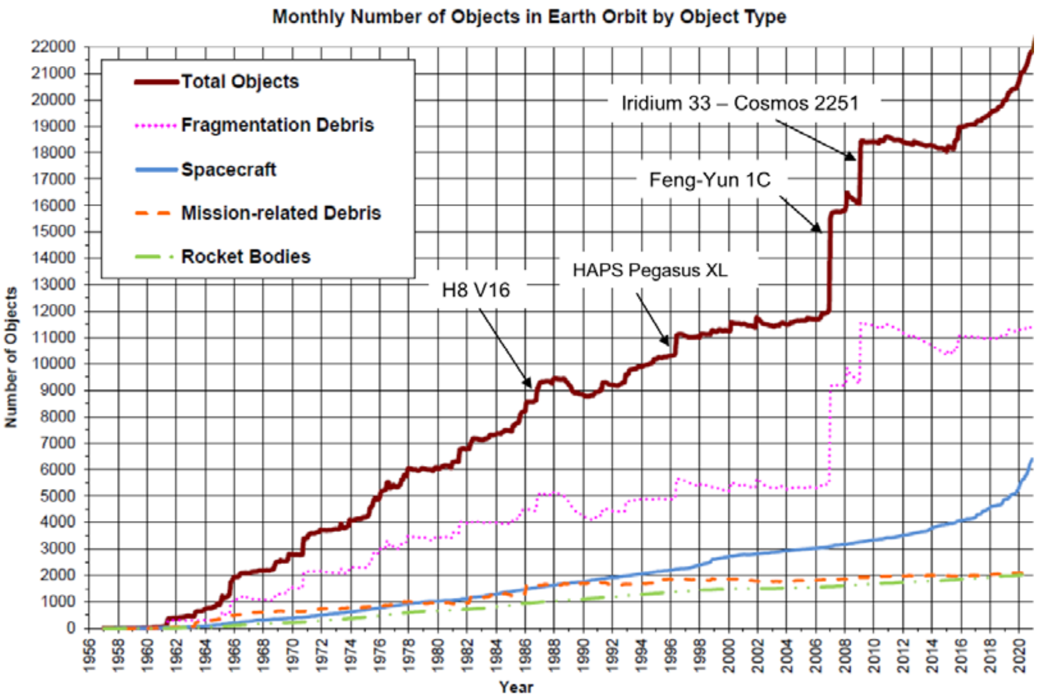

Fig. 1. Debris evolution over time. In early 2021, 36,000 orbital objects were present, of which 24k were catalogued, 94 % of these being debris. Even more are present since the recent experiments demonstrating satellite targeting from Earth [courtesy NASA Orbital Debris Program Office, 2020]. Shown are just the debris larger than 10 cm.

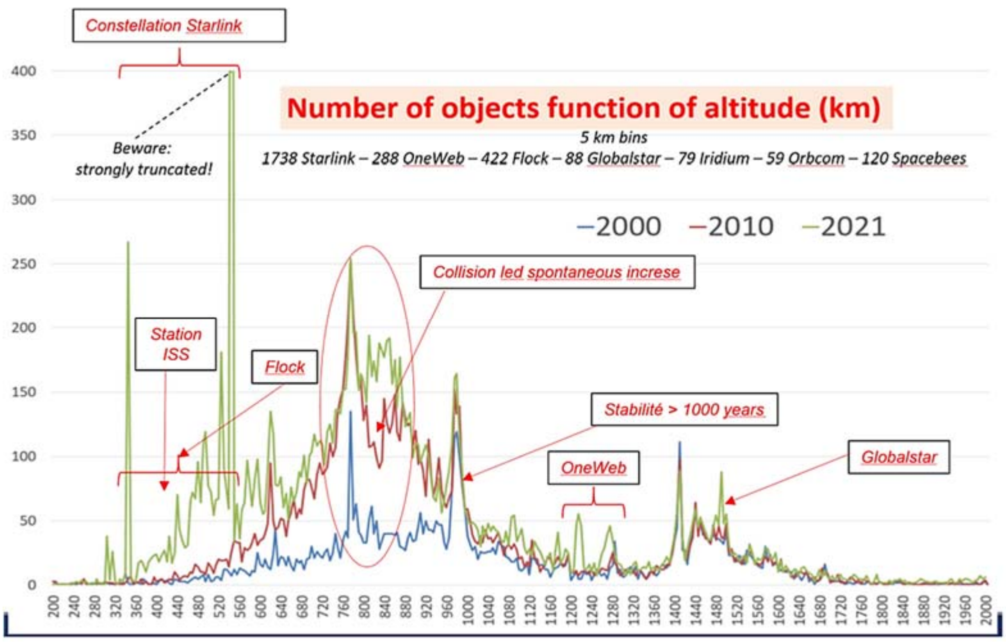

Fig. 2. Debris number in various altitude bins [Courtesy of C. Bonnal].

Then, we can use pulses from a high power laser on the same or a different spaceborne station to nudge one partner in a predicted collision via laser ablation a few days in advance and avoid the collision. Increased orbit precision resulting from laser ranging will permit collision avoidance by imparting a velocity of about 0.15 mm/s 7 days in advance to the selected partner, sufficient to miss the anticipated collision by 280 m.

Fig. 3 illustrates the severity of the debris problem. This figure is a computer-generated image of tracked objects larger than 10 cm in modern times, as viewed from an oblique vantage point in high earth orbit (HEO). 95 % of objects shown are debris, not functional satellites. The cloud is very dense in LEO, but the geosynchronous space (GEO) is also getting crowded. Note the number of objects that exist outside the GEO ring.

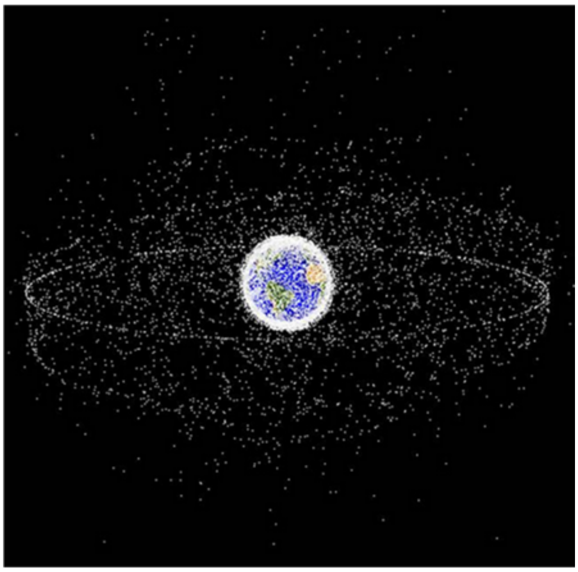

Fig. 3. Illustrating the debris problem (NASA Orbital Debris Program Office, 2020).

2. Precise Object Location

Fig. 4 shows the design of an orbiting telescope and high-efficiency detector system, designed to detect debris objects (>10 cm at 1000 km range, >1 cm at 200 km) under solar illumination.

After a debris is detected, 50 mJ, 100 ps laser pulses are trained on it to measure range to the object with 4 cm precision by timing reflections from tracked objects (Fig. 5). In active mode, it can see a 20 cm target at 1000 km and a 6cm target at 200 km.

Tables 1-3 summarize system performance. Several systems like that shown in Fig. 4 and Fig. 5, moving in equatorial and polar orbits at ~900 km altitude gather data on the debris surface from multiple passes of multiple stations per object. Then, a computer on a "mother ship" will determine the center of mass location of each object studied with 10 cm precision. In Table 1, we assume the minimum signal integration time (60 microseconds per pixel) and a 1ms refresh interval during which noise energy accrues. Table 1 shows system performance in passive target detection, in the solar illuminated mode illustrated in Fig. 4. At 1000 km range, a LEO object moving across the field of view will cross the 1-degree field of view in about 2 s. The 1.54 Gpixel array covers a 40 × 40 km field at 1000 km with 230 cm spot size [Fig. 5]. The pixels have 85 % photoelectric efficiency [7]. Dark current is adequate at 20C. A commercial laser which satisfies our requirements is the EKSPLA PL2231A, which cost about $135k in 2020 [8].

Background signal assumes we are in LEO above 300 km, sun behind us, and looking up or out, but not down at Earth. Background brightness is based on 1 μW/(m^2sterradian-μm) [9]. Tables 2 and 3 show ranging laser performance in active mode.

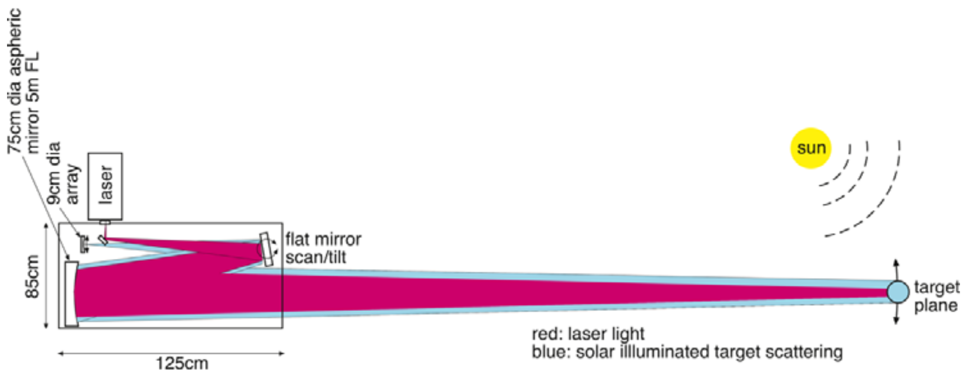

Fig. 4. Passive and active components of LEO ranging system to detect large debris using solar illumination followed by 100 ps "pinging." Operation is illustrated at 100 km range, where laser spot size is smaller than large targets.

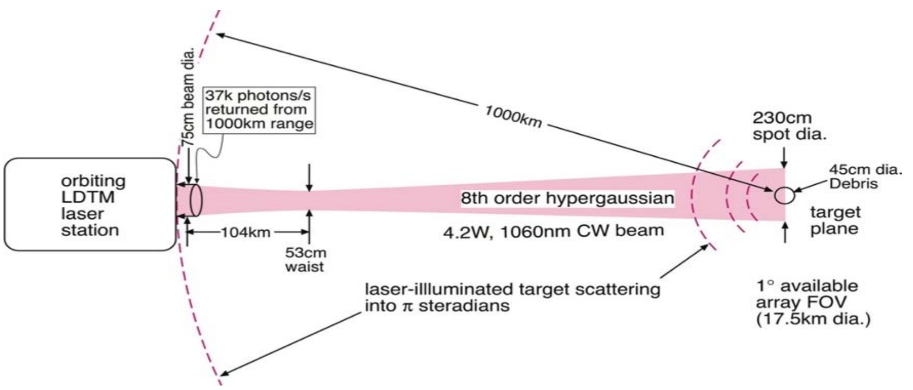

Fig 5. Active ranging subsystem comprising a 50 mJ, 100 ps laser and precision timer to determine range to debris with cτ=3 cm precision. Here, operation at 1000 km range is illustrated, with beamwaist at 104 km.

Table 1. Passive mode: sun-illuminated LEO target.

	Value	Dimension
Operating range	1000	km
Sun spectral brightness	1000	W/(m²sterrad- µm)
Background spect. bright	1E-6	W/(m²sterrad- µm)
Relativistic shift BW	0.025	nm
Target size assumed	10	cm
Range assumed	1000	km
Min. transit time/pixel	60	µs
Aperture diameter	85	cm
Target $R_{diffuse}$	0.25	-
Signal S	1.7E-17	W
Noise N	1.0E-16	W
Signal energy	3.0E-15	J
Background energy	5.8E-22	J
Array refresh interval	1	ms
Signal/Noise energy ratio	2.8E4	-
Photoelectrons/pixel	38	-

Table 2. Ranging laser parameters.

	Value	Dimension
Wavelength	532	nm
Pulse energy	50	mJ
Pulse duration	100	ps
Repetition rate	50	Hz
Laser avg. power	2.5	W
Laser beam quality M^2	2	-

Table 3. Ranging laser active detection system parameters.

	Value	Dimension
Center wavelength	532	nm
Aperture diameter D	85	cm
Target diameter d	20	cm
Target diffuse reflectivity R_d	25	%/sterrad
Beam dia. (0.9*D)	75	cm
Focal length	5	m
Field of view	1	deg
Search area	1600	km²
N pixels	1.54E9	-
Pixel size	2.25	µm
Array diameter (concave)	8.7	cm
Detector efficiency	85	%
Received signal S	1.3E-17	J
Refresh time	1	ms
Background B (gated)	4.4E-23	J
Spot diameter at range	2.3	m
Target diffuse reflectivity	0.25	-
S/B	3.0E6	-
Target $v_\perp$ at range	7500	m/s
Min transit time/pixel	60	µs
Rec'd photo-electrons	30	-
Signal stability $1/N_{pe}^{0.5}$	18	%
Min target at 208 km	6.5	cm
Dark current at 20C	0.3	e/pulse/ms

3. Diffraction

Please refer to Fig. 5. For long range systems such as ours, the place to start is the beam diameter at the launch aperture. From Table 3, this is 75 cm. Next, the Rayleigh Range (the position at which intensity is doubled for a Gaussian beam) is determined, from

$$z_R = \frac{\pi w_o^2}{M^2 \lambda}, \quad (1)$$

which gives us the distance from the beamwaist to the aperture. W_o is the waist radius. Note that a beam with quality M^2 behaves just like a beam with wavelength $M^2\lambda$. Beyond the waist, as the beam expands at range $z' = z - z_R$ we can write without approximation:

$$w^2 = w_o^2[1+(z'/z_R^2)] \quad (2)$$

From this result, we know the beam area $A=\pi w^2$ on the target and can compute fluence $\Phi=W/A$ where W is pulse energy. To compute the return energy, we assume a pulse energy $R_d W$ is returned into π sterradians. This approach is a worst case, because most objects have roughly flat surfaces that return light into a much narrower beam than we assumed in calculating he parameters in Fig. 5 and Table 3.

4. Nudging the Target

Fig. 6 illustrates nudging a target satellite. The Fig. 4 system is collinear with the Fig. 6 high power, single pulse high energy laser. This laser can apply its Δv from hundreds of km, providing intensity on target is sufficient to produce a plasma and initiate ablation. The requirements for that are a fluence value [10].

$$\Phi_{opt} \sim B\sqrt{\tau}\ \mathrm{J/m^2} \quad (3)$$

We take $B=4.0E8\ \mathrm{J/m^2}$ for robust coupling to most spacecraft materials at pulse duration τ, giving $\Phi_{opt}=4.0\ \mathrm{kJ/m^2}$ in a 100 ps pulse. §3 can be used to determine fluence at range. In Fig. 6, "L'ADROIT" refers to an orbiting debris removal station design [10].

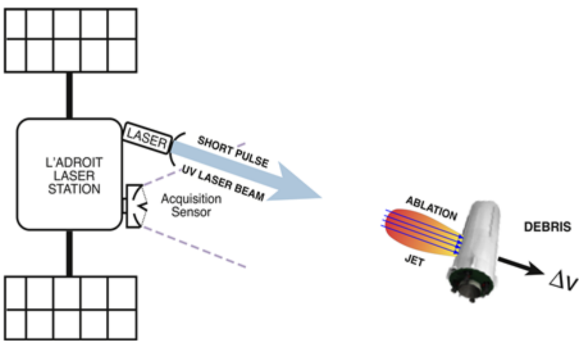

Fig. 6. Illustrating debris nudging.

4.1. Perturbing Orbits

Where $\mu = GM_{Earth}$, r is radius from the elliptical orbit focus (geocentric radius for small satellites) and a is the semi-major axis of the ellipse, total energy per unit mass ε for an unperturbed orbit is given by

$$\varepsilon = v_{orb}^2 / 2 - \mu / r = -\mu / 2a \qquad (4)$$

The vis viva equation for velocity *v* in an unperturbed orbit is

$$v^2 = \mu(2/r - 1/a) \qquad (5)$$

If we now perturb the orbit with a laser impulse with energy W which delivers an energy change $C_m W v_{orb}$ we can differentiate Eq. (5) to find for an object of mass m,

$$\Delta\varepsilon = \pm(\frac{\mu}{2a^2})\Delta a = C_m W v_{orb} / m \qquad (6)$$

Considering that the orbital period is given by

$$T = 2\pi a^{3/2} / \mu^{1/2} \qquad (7)$$

which can be differentiated to give

$$\Delta T = 3\pi(a/\mu)^{1/2}\Delta a$$

so that

$$\Delta T = 3\pi(a/\mu)^{1/2}(\frac{2a^2}{\mu}\Delta\varepsilon) = (3aT/\mu)\Delta\varepsilon$$

and that the change in period of the perturbed object is

$$\Delta T = \pm 6\pi W C_m(\frac{a^2}{\mu M}) \qquad (8)$$

Eq. (8) works even for a CW signal if its duration is short compared to T. But W in Eq. (8) must always be used with the correpondng C_m.

Table 4 shows how we can apply all this. Please note that this high power pulse laser, is a separate device from the 50 mJ unit in Table 2, and makes only one shot to produce a 280 m miss in 7 days, giving it a lot of flexibility to address many targets. Its 800 km range addresses a large enough volume to find a particular debris quickly. Note that focal spot position dither means nothing for a 100 ps pulse focal spot fluence. No vibrations are that fast.

We suggest that the 3 m diameter focusing aperture can be a phase plate imprinted on a flat reflector simulating an off-axis paraboloid and assembled from segments in orbit. Secondary optics in the laser train feeding this optic adjust the focus location in real time within the indicated range. At shorter range, laser pulse energy is reduced. Coupling coefficient values in Table 4 were estimated from earlier measurements [11]. Pointing precision is referenced in [12].

Table 4. Target mechanical coupling parameters.

	Value	Dimension
Coupling coefficient C_m	30E-6	N-s/J
Wavelength	355	nm
Aperture diameter	3.0	m
Beam quality M^2	1.5	-
Focal spot dia. at range	40	cm
Range	800	km
Pointing precision	300	nrad
Corresponding focus dither	24	cm
Target mass	1000	kg
Nudging laser energy	5.0	kJ
Fluence on target	40	kJ/m^2
Target Δv from one shot	150	µm/s
Target ΔT	3.9	ms/orbit
Pulse duration	100	ps
Semimajor axis change Δa	±29	cm
Miss distance v_{orb} ΔT	2.8	m/period
Miss distance v_{orb} ΔT	280	m/week

4.2. Design of a JCA Station

Fig. 7 shows a polar orbiting JCA station in action.

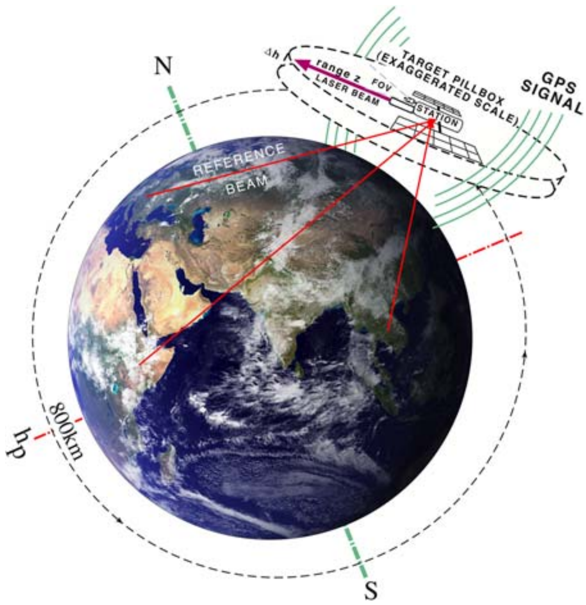

Fig. 7. Polar orbiting JCA Station.

In operation, this 100 ps laser ranging station (one of many) accurately locates a debris facet relative to the station. In turn, the station is located relative to Earth by onboard GPS and multiple Earth stations pinging a retroreflector on the station.

Using inputs from many stations, a computer on the "mother ship" combines the data to determine the center of mass location of a particular debris with 10 cm precision. In Table 5, we take 19,000 satellites to be surveyed by an individual JCA station, and 0.1 % of these to require special care because of their proximity to other assets. Ten stations in various equatorial or polar orbits can provide redundant measurements for those, getting center of mass location accurately.

Table 5. JCA system parameters.

	Value	Dimension
Altitude h	800±50	km
Orbit period T	101	min
Pillbox thickness	600	km
Pillbox volume V	1.88E9	km^3
Number satellites watched	19000	-
Satellite density	6.2E-8	km^{-3}
Target objects in pillbox	120	-
Watched sat detection rate	4700	hr^{-1}
Sats to nudge (0.1% /day)	1	day^{-1}
Time to find a particular sat	4	hrs

5. Alternative Designs

In this section, we will compare earth-based and space-based ranging systems in order to show the inherent advantages of the pulsed system we propose, and briefly discuss CW laser ranging with frequency modulation, the design approach used in automobile collision-avoidance lidar.

5.1. CW Laser Ranging?

Using the same geometry and procedures as generated Fig. 5 and Table 1, we can calculate that to obtain the same spectral brightness as the sun (Table 1) on target, a 532 nm CW laser with 100 nm bandwidth and 1.3 kW output would be required. This figure could be improved by shifting the frequency of the transmitted signal in a pseudorandom sequence that repeats every 3.3 ms (to match 1000 km range) and cross-correlating the return with the outgoing signal. However, there are other problems with CW.

In order to provide the 0.15N-s impulse necessary to nudge the target (see Table 4) using light pressure alone, for which C_m=6.7E-9N/W, assuming a target availability interval of 30 s, a laser power of 750 kW would be needed. At 25 % electrical efficiency for the laser, a power supply capable of 3MW is necessary. Over the 30 s availability interval, 90MJ stored electrical energy would be required. These parameters are not practical.

5.1. Ground-based Laser Ranging?

Problems are both physical and practical (Table 6). Clearly, it would take a lot of fixed Earth-based stations to equal the capability of one orbiting station.

Because sky background brightness is more than 100 times greater for an Earth-based station, small targets would be much more difficult to find.

Table 6. Earth-based laser ranging.

	Earth	Space
Search volume (±45°) km^3	1.4E9	1.9E9
Sky background brightness	7.5E-9	1E-6
Time to find one satellite	2 weeks*	4 hrs
Weather a problem?	Yes	No
Scintillation (adaptive optics)	Yes	No
Nonlinear refraction	Yes	No
Centimetric precision	No	Yes
Operating time (hrs)	12	24

Note: * depends critically on satellite orbit and station location – could be infinite.

6. Stepwise Approach

Because many nations' properties are involved in the space commons, an attempt to range, let alone nudge satellites requires careful planning and international consultation. To do this will require a multi-year program. We propose the following sequence:

1. Develop a small laser ranger for demonstration purposes.
2. At first, use this only on large known French debris such as Ariane 1-4 upper stages.
3. Compare results to the well-known ephemerii from the French COSMOS system based on the Graves radar [13].
4. When feasibility is proven, develop larger laser ranging station compatible in size with the European Vega launcher.
5. Develop a global legal agreement to allow laser ranging on catalogued debris. Gains from such operations on defunct objects should guarantee acceptance.
6. Because known ephemerii will control the initial operation, the risk of wrongly pinging active assets is negligible.
7. Develop the slightly larger JCA system couple with the ranging function to minimize the false alarm rate.
8. When feasibility of this is shown, use the JCA system to significantly modify orbits of large derelicts as previously proposed in the description of L'ADROIT [10, 14].

7. Conclusions

It has been the purpose of this paper to outline a practical solution to abating the problem of mutual collisions among satellites before we are trapped on this planet by a cloud of debris created by these collisions. The plan is to locate all objects in LEO sufficiently precisely to avoid false collision alarms and to predict actual collisions several days in advance. Armed with this knowledge, we can use a nudging laser system which, by imparting a tiny velocity change a week in advance, will eliminate collisions altogether.

Acknowledgements

We gratefully acknowledge the encouragement of Prof. Dr. Sergey Yurish of IFSA to produce this paper.

References

[1]. I. Klotz, Starlink Satellites Interfering with Astronomical Observations, *Aviation Week and Spase Technology,* 5 March 2020.

[2]. H. Klinkrad, Space Debris: Models and Risk Analysis, *Springer Praxis Books*, 2006.

[3]. D. J. Kessler, B. G. Cour-Palais, Collision Frequency of Artificial Satellites: The Creation of a Debris Belt, *J. Geophys. Res.*, Vol. 83, Issue A6, 1978, pp. 2637-2646.

[4]. C. Smith, Remote manoeuvre of space debris using photon pressure for active collision avoidance, in *Proceedings of the 5th European Workshop on Space Debris Modeling and Remediation,* 2018, Paper 7.2.

[5]. C. Bonnal, D. McKnight, C. Phipps, C. Dupont, S. Missonnier, L. Lequette, M. Merle, S. Rommelaere, Just in time collision avoidance – a review, *Acta Astronautica,* Vol. 170, 2020, pp. 637-651.

[6]. H. Krag, *et al*., Groundbased laser for tracking and remediation – an architectural view, paper IAC-18-A6.7.1, in *Proceedings of the* 69th *International Astronautical Congress (IAC'2018)*, Bremen, 2018.

[7]. Based on published specifications of Fairchild Imaging CCD456 (1 nA/cm^2)

[8]. S. Guthrie, Altos Photonics, *Private Communication*, 25 June 2019.

[9]. Ch. Leinert, *et al*., The 1997 reference of diffuse night sky brightness, *Astron. Astrophys. Suppl. Ser*., Vol. 127, 1998, pp. 1-99.

[10]. C. Phipps, L'ADROIT – A spaceborne ultraviolet laser system for space debris clearing, *Acta Astron.,* Vol. 104, 2014, pp. 243-255.

[11]. C. R. Phipps, M. Boustie, J.-M. Chevalier, S. Baton, E. Brambrink, L. Berthe, M. Schneider, L. Videau, S. A. E. Boyer, S. Scharring, Laser Impulse Coupling measurements at 400 fs and 80 ps using the LULI facility at 1057 nm wavelength, *J. Appl. Phys.*, Vol. 122, 2017, 193103.

[12]. M. Aguirre, J.-L. Bezy, ESA activities related to high resolution imaging from GEO, *ESRIN*, 15 April 2010, page 51.

[13]. IAA Situation Report on Space Debris, http://www.iaaweb.org/iaa/Scientific%20Activity/sg514finalreport.pdf

[14]. C. Phipps, C. Bonnal, A spaceborne, pulsed UV laser system for re-entering or nudging LEO debris, and re-orbiting GEO debris, *Acta Astronautica*, Vol. 118, 2016, pp. 224-236.